

Production of para– and orthopositronium at relativistic heavy ion colliders

G. L. Kotkin*

Department of Physics, Novosibirsk State University, Novosibirsk, 630090, Russia

E. A. Kuraev†

Laboratory of Theoretical Physics, Joint Institute for Nuclear Research, Dubna, 141980 Russia

A. Schiller‡

Institut für Theoretische Physik and Naturwissenschaftlich-Theoretisches Zentrum, Universität Leipzig, D-04109 Leipzig, Germany

V. G. Serbo§

Department of Physics, Novosibirsk State University, Novosibirsk, 630090, Russia

(November 27, 1998)

Abstract

We consider the ortho– and parapositronium production in the process $AA \rightarrow AA + Ps$ where A is a nucleus with the charge number Z. The inclusive cross section and the energy distribution of the relativistic Ps are calculated which are of primary interest from the experimental point of view. The accuracy of the corresponding cross sections is given by omitting terms $\sim (Z\alpha)^2/L^2$ for the para–Ps and $\sim (Z\alpha)^2/L$ for the ortho–Ps production where $L = \ln \gamma^2 \approx 9$ and 16 for the RHIC and the LHC. Within this accuracy the multiphoton (Coulomb) corrections are taken into account. We show that the RHIC and the LHC will be Ps factories with a productions rate of about $10^5 \div 10^8$

*Email address: kotkin@math.nsc.ru

†Email address: kuraev@thsun1.jinr.dubna.su

‡Email address: schiller@tph204.physik.uni-leipzig.de

§Email address: serbo@math.nsc.ru

relativistic Ps per day. The fraction of the ortho-Ps is expected to be of the same order as that of the para-Ps for Au–Au and Pb–Pb collisions.

PACS numbers: 25.75-q, 36.10.Dr, 12.20.-m

I. INTRODUCTION.

Parapositronium (para-Ps, n^1S_0) has a positive charge parity $C = +1$ and in the ground state, $n = 1$, its life time at rest τ_0 is $c\tau_0 = 3.7$ cm. On the other hand, orthopositronium (ortho-Ps, n^3S_1) has $C = -1$ and $c\tau_0 = 42$ m. The relativistic Ps has a decay length $c\tau_0\varepsilon/m_{\text{Ps}}$ where ε and $m_{\text{Ps}} \approx 2m_e$ denote its energy and mass. The production of Ps in different collisions is of interest by the following reasons:

- Ps can be used to test fundamental laws like the *CPT*-theorem (see review [1]).
- A more detailed comparison between the experimental value of ortho-Ps width and its theoretical prediction is necessary since up to now there is an essential difference between them [2]).
- Relativistic Ps can be used to study the unusual large transparency of Ps in thin layers predicted in Refs. [3,4].

Up to now the following methods have been proposed to create positronium: The photo-[5]- [8] and electroproduction [5,9,10] of Ps on nuclei and atoms. The results of Refs. [5]- [10] were completed and corrected in Ref. [11]. Recently a new method, based on an electron cooling technique, was proposed in the works [1,12]. It was claimed that this method can give about 10^4 nonrelativistic Ps per second on a specifically designed accelerator.

In the present paper we study in detail a new and promising possibility — the production of relativistic Ps at colliders with relativistic heavy nuclei like the RHIC and the LHC, i.e. we consider the process $AA \rightarrow AA + \text{Ps}$ where A denotes the nucleus with charge number Z . The parameters of these colliders (from Refs. [13]) are given in Table I. We show that at these colliders

$$\sim 1 \div 10^3 \text{ relativistic Ps per second} \quad (1.1)$$

will be produced. It is interesting to note that the ratio of ortho-Ps to para-Ps events turns out to be large: for the RHIC about 0.8, for the LHC 0.3 in the Pb-Pb mode and 0.02 in the Ca-Ca mode.

Up to now only the total cross section for para-Ps production has been calculated in the leading logarithmic approximation (LLA) (see Ref. [5]). There it has been found:

$$\sigma_{\text{para}}^{\text{LLA}} = \frac{1}{3} \zeta(3) \sigma_0 L^3, \quad \sigma_0 = \frac{Z^4 \alpha^7}{m_e^2}, \quad \zeta(3) = \sum_{n=1}^{\infty} \frac{1}{n^3} = 1.202 \dots, \quad L = \ln \gamma^2. \quad (1.2)$$

However, for experiments (especially with relativistic Ps), it is much more interesting to know the energy and angular distributions of Ps which are given by the inclusive cross section and energy spectrum of Ps. These distributions for para-Ps as well as for ortho-Ps are calculated in the present work. In our calculations we also take into account with a certain accuracy the Coulomb correction (CC) related to multiphoton exchange of the produced Ps with nuclei described by Feynman diagrams of Fig. 1. They are quite important and decrease the cross sections by $30 \div 50$ % for the Au-Au and Pb-Pb collisions. The approach used here is based essentially on results on the production of relativistic positronium in collisions of photons and electrons with heavy ions presented in our recent work [11].

Our main notations are given in Eq. (1.2) and Fig. 1: the i -th nucleus changes its 4-momentum (energy) P_i (E) to P'_i (E'_i) and emits n or n' virtual photons with the total 4-momentum $q_i = P_i - P'_i$ and the energy $\omega_i = E - E'_i$. These photons collide and produce Ps with 4-momentum $p = q_1 + q_2$ and energy $\varepsilon = \omega_1 + \omega_2$. Due to charge parity conservation, the sum $n + n'$ is even (odd) for para-Ps (ortho-Ps) production. We use the c.m.s. with the z -axis along the vector \mathbf{P}_1 and denote by \mathbf{p}_\perp the transverse components of vector \mathbf{p} . The CC depends on the parameter

$$\nu = Z\alpha \approx Z/137. \quad (1.3)$$

In Section 2 we discuss the production of para-Ps in ultrarelativistic heavy ion collisions. After selecting the leading diagrams including the multiphoton exchange with the nuclei, the Born cross sections are calculated in the equivalent photon approximation to identify the dominant kinematical regions. The exact Born cross sections for ultrarelativistic ions are found in the next subsection. The CC are calculated in the accuracy given by the selection of the leading diagrams. Section 3 is devoted to the production of ortho-Ps. Our results are summarized in Section 4 where we discuss the expected production rates for the colliders RHIC and LHC.

II. PRODUCTION OF PARA-PS

A. Selection of the leading diagrams including the multiphoton exchange

The amplitude M_{para} of the para-Ps production can be presented in the following form via the sums over amplitudes $M_{nn'}$ of Fig. 1 (with $n + n'$ being even)

$$M_{\text{para}} = \sum_{n,n' \geq 1} M_{nn'} = M_B + M_1 + \tilde{M}_1 + M_2, \quad M_B \equiv M_{11}, \quad (2.1)$$

$$M_1 = \sum_{n'=3,5,7,\dots} M_{1n'}, \quad \tilde{M}_1 = \sum_{n=3,5,7,\dots} M_{n1}, \quad M_2 = \sum_{n,n' \geq 2} M_{nn'}.$$

Here M_B is the Born amplitude in which each nucleus emits one photon, the item M_1 (\tilde{M}_1) corresponds to the case when the first (second) nucleus emits one photon while the other nucleus emits at least three photons, the last term M_2 corresponds to the case when both nuclei emit at least two photons. Using this decomposition of the amplitude, we present the cross section in the form

$$\sigma_{\text{para}} = \sigma_B + \sigma_1 + \tilde{\sigma}_1 + \sigma_2, \quad d\sigma_B \propto |M_B|^2,$$

$$d\sigma_1 \propto 2\text{Re}(M_B M_1^*) + |M_1|^2, \quad d\tilde{\sigma}_1 \propto 2\text{Re}(M_B \tilde{M}_1^*) + |\tilde{M}_1|^2, \quad (2.2)$$

$$d\sigma_2 \propto 2\text{Re}(M_B M_2^* + M_1 \tilde{M}_1^* + M_1 M_2^* + \tilde{M}_1 M_2^*) + |M_2|^2.$$

It is not difficult to estimate that the integration over the total virtual photon momenta squared q_1^2 and q_2^2 gives two large Weizsäcker–Williams (WW) logarithms $\sim L^2$ in σ_B , one large WW logarithm $\sim L$ in σ_1 and $\tilde{\sigma}_1$ and no one large WW logarithm in σ_2 . Therefore, the relative contributions of the items σ_i is $\sigma_1/\sigma_B = \tilde{\sigma}_1/\sigma_B \sim \nu^2/L$ and

$$\frac{\sigma_2}{\sigma_B} \sim \frac{\nu^2}{L^2} < 0.4\% \quad (2.3)$$

for the colliders in Table I. As a result, with an accuracy of the order of 1 % we can neglect σ_2 and use the equation

$$\sigma = \sigma_B + \sigma_1 + \tilde{\sigma}_1. \quad (2.4)$$

Moreover, with the same accuracy we can calculate σ_1 and $\tilde{\sigma}_1$ in LLA only since the terms next to the leading ones are of the order of ν^2/L^2 .

B. Calculating the Born cross section in the equivalent photon approximation

Before we proceed to a more exact calculation of $d\sigma_B$, it is useful to perform a rough estimate using the equivalent photon approximation (EPA). This allows us to identify the dominant region in phase space.

It is well known that the main contribution to the pair production $AA \rightarrow AAe^+e^-$ is given by the region of small photon virtualities $-q_i^2 \ll (q_1 + q_2)^2$. Therefore, for the Ps production this region is¹

$$-q_i^2 \ll 4m_e^2, \quad (2.5)$$

i.e. the virtual photons are almost real in the dominant region. Since

$$-q_i^2 = \mathbf{q}_{i\perp}^2 + (\omega_i/\gamma)^2, \quad (2.6)$$

we immediately conclude that in the dominant region the photon energies ω_i are small compared with the nucleus energies E :

$$\omega_i \lesssim m_e\gamma \ll E. \quad (2.7)$$

In the EPA the cross section for the $AA \rightarrow AA + \text{Ps}$ process is related to the cross section for the real photoprocess $\gamma\gamma \rightarrow \text{Ps}$ by

$$d\sigma_B = dn_1(\omega_1) dn_2(\omega_2) \sigma_{\gamma\gamma \rightarrow \text{Ps}}(\omega_1\omega_2), \quad \omega_{1,2} \approx \frac{1}{2}(\varepsilon \pm p_z), \quad (2.8)$$

where dn_i is the number of the equivalent photons generated by the i -th nucleus. For dn_i we use two equivalent forms (see, for example, formulae from Appendix D of review [14] in which we omit terms of the order of ω_i/E (in virtue of relation (2.7))

$$dn_i = \frac{Z^2\alpha}{\pi^2} \frac{\mathbf{q}_{i\perp}^2}{(q_i^2)^2} \frac{d\omega_i}{\omega_i} d^2q_{i\perp}, \quad (2.9)$$

¹This can also be seen from the expression for the Born amplitude obtained in Appendix A.

$$dn_i = \frac{Z^2\alpha}{\pi} \left[1 - \frac{(\omega_i/\gamma)^2}{(-q_i^2)} \right] \frac{d\omega_i}{\omega_i} \frac{d(-q_i^2)}{(-q_i^2)} \frac{d\varphi_i}{2\pi}, \quad (2.10)$$

where φ_i is the azimuthal angle of the vector \mathbf{q}_i . It is also well known that the equivalent photons of small energy are completely linearly polarized in the scattering plane and their polarization vectors are

$$\mathbf{e}_i = \frac{\mathbf{q}_{i\perp}}{|\mathbf{q}_{i\perp}|}. \quad (2.11)$$

The cross section for the real photoprocess $\gamma\gamma \rightarrow \text{Ps}$ can be easily obtained using the known width of the $n \ ^1S_0$ state $\Gamma_{\text{Ps} \rightarrow \gamma\gamma} = \alpha^5 m_e (\mathbf{e}_1 \times \mathbf{e}_2)^2 / (4n^3)$ and summing over all para-Ps states n

$$\sigma_{\gamma\gamma \rightarrow \text{Ps}} = 4\pi^2 \alpha^5 \zeta(3) (\mathbf{e}_1 \times \mathbf{e}_2)^2 \delta(4\omega_1\omega_2 - 4m_e^2). \quad (2.12)$$

Substituting Eqs. (2.10)-(2.12) into (2.8) and integrating over φ_i , ω_2 and over q_i^2 in the region

$$(\omega_i/\gamma)^2 \lesssim -q_i^2 \lesssim m_e^2 \quad (2.13)$$

we find with logarithmic accuracy

$$d\sigma_B = 2\zeta(3)\sigma_0 \ln \frac{m_e\gamma}{\omega_1} \ln \frac{m_e\gamma}{\omega_2} \frac{d\omega_1}{\omega_1}, \quad \omega_1\omega_2 \approx m_e^2. \quad (2.14)$$

Taking into account the inequalities (2.7), we conclude that the main region for ω_1 is

$$\frac{m_e}{\gamma} \lesssim \omega_1 \lesssim m_e\gamma. \quad (2.15)$$

Integrating $d\sigma_B$ (2.14) over the photon energy ω_1 in the region (2.15) we obtain the total cross section (1.2).

The **spectrum** of the relativistic Ps can be obtained from Eq. (2.14) as follows. Let us divide the region (2.15) into two symmetrical subregions. In the first one, $m_e \ll \omega_1 \lesssim m_e\gamma$, we have $\omega_1 \approx \varepsilon \approx p_z$, $\omega_2 \approx m_e^2/\varepsilon$ and the contribution to the spectrum is

$$d\sigma_B^{(1)} = 2\zeta(3)\sigma_0 \ln \frac{m_e\gamma}{\varepsilon} \ln \frac{\varepsilon\gamma}{m_e} \frac{d\varepsilon}{\varepsilon}. \quad (2.16)$$

In the second subregion $m_e/\gamma \lesssim \omega_1 \ll m_e$ we have $\omega_2 \approx \varepsilon \approx -p_z$, $\omega_1 \approx m_e^2/\varepsilon$ and

$$d\sigma_B^{(2)} = 2\zeta(3)\sigma_0 \ln \frac{\varepsilon\gamma}{m_e} \ln \frac{m_e\gamma}{\varepsilon} \frac{d\varepsilon}{\varepsilon}. \quad (2.17)$$

The total contribution of these two subregions is

$$d\sigma_B = 4\zeta(3)\sigma_0 \ln \frac{m_e\gamma}{\varepsilon} \ln \frac{\varepsilon\gamma}{m_e} \frac{d\varepsilon}{\varepsilon}, \quad m_e \ll \varepsilon \lesssim m_e\gamma. \quad (2.18)$$

Integrating this spectrum over ε leads to the result (1.2).

To calculate the **inclusive cross section** we substitute Eqs. (2.9), (2.11), (2.12) into (2.8) and perform a simple integration

$$\int \frac{d\omega_1}{\omega_1} \frac{d\omega_2}{\omega_2} \delta(4\omega_1\omega_2 - 4m_e^2) = \frac{1}{4m_e^2} \frac{dp_z}{\varepsilon}.$$

Further, we insert into the right-hand side of Eq. (2.8) the factor

$$1 = \int \delta(\mathbf{q}_{1\perp} + \mathbf{q}_{2\perp} - \mathbf{p}_\perp) d^2p_\perp$$

and find the inclusive cross section in the form

$$\varepsilon \frac{d^3\sigma_B}{d^3p} = \frac{\zeta(3)}{\pi^2} \sigma_0 \int \frac{(\mathbf{q}_{1\perp} \times \mathbf{q}_{2\perp})^2}{(q_1^2 q_2^2)^2} \delta(\mathbf{q}_{1\perp} + \mathbf{q}_{2\perp} - \mathbf{p}_\perp) d^2q_{1\perp} d^2q_{2\perp}. \quad (2.19)$$

From this expression and taking into account Eqs. (2.6), (2.13), we conclude that the leading logarithmic contribution to the cross section is given by the region

$$\left(\frac{\omega_1}{\gamma}\right)^2 + \left(\frac{\omega_2}{\gamma}\right)^2 \ll \mathbf{p}_\perp^2 \ll m_e^2. \quad (2.20)$$

It arises from the two symmetrical subregions:

$$\begin{aligned} \left(\frac{\omega_1}{\gamma}\right)^2 &\ll \mathbf{q}_{1\perp}^2 \ll \mathbf{p}_\perp^2, & \mathbf{q}_{2\perp} &\approx \mathbf{p}_\perp, \\ \left(\frac{\omega_2}{\gamma}\right)^2 &\ll \mathbf{q}_{2\perp}^2 \ll \mathbf{p}_\perp^2, & \mathbf{q}_{1\perp} &\approx \mathbf{p}_\perp. \end{aligned} \quad (2.21)$$

The contribution from the first region is

$$\frac{\zeta(3)}{2\pi^2} \sigma_0 \int_0^{2\pi} d\varphi \int_{(\omega_1/\gamma)^2}^{p_\perp^2} d\mathbf{q}_{1\perp}^2 \frac{(\mathbf{q}_{1\perp} \times \mathbf{p}_\perp)^2}{(\mathbf{q}_{1\perp}^2 \mathbf{p}_\perp^2)^2} = \frac{\zeta(3)}{2\pi} \frac{\sigma_0}{\mathbf{p}_\perp^2} \ln \frac{\mathbf{p}_\perp^2 \gamma^2}{\omega_1^2}.$$

Taking into account the second region, we find the whole inclusive cross section

$$\varepsilon \frac{d^3\sigma_B}{d^3p} = \frac{\zeta(3)}{\pi} \frac{\sigma_0}{\mathbf{p}_\perp^2} \ln \frac{\mathbf{p}_\perp^2 \gamma^2}{m_e^2}. \quad (2.22)$$

Integrating this expression over \mathbf{p}_\perp^2 in the range (2.20) and taking into account the two symmetrical subregions (2.16,2.17) mentioned before, we obtain the spectrum (2.18).

C. The exact calculation of the Born cross section for ultrarelativistic ions

The Born amplitude of the discussed process is obtained in Appendix A omitting terms of the relative order of $1/\gamma^2$, m_e/M or smaller. Using this expression for the amplitude we can present the **inclusive cross section** in the form

$$\varepsilon \frac{d^3\sigma_B}{d^3p} = \frac{\zeta(3)}{4\pi} \frac{\sigma_0}{m_e^2} J_B, \quad (2.23)$$

$$J_B = \frac{4m_e^2}{\pi} \int \mathbf{A}^2 \delta(\mathbf{q}_{1\perp} + \mathbf{q}_{2\perp} - \mathbf{p}_\perp) d^2q_{1\perp} d^2q_{2\perp},$$

$$\mathbf{A} = \frac{\mathbf{q}_{1\perp} \times \mathbf{q}_{2\perp}}{q_1^2 q_2^2} \frac{4m_e^2}{4m_e^2 - q_1^2 - q_2^2}$$

which differs from the approximate Eq. (2.19) only by the factor $(4m_e^2)^2/(4m_e^2 - q_1^2 - q_2^2)^2$ in the integrand. It is convenient to introduce the dimensionless variables

$$x = \frac{\varepsilon + p_z}{4m_e\gamma}, \quad \tilde{x} = \frac{\varepsilon - p_z}{4m_e\gamma}, \quad \tau = \left(\frac{\mathbf{p}_\perp}{2m_e} \right)^2. \quad (2.24)$$

They are not independent, but connected by the constraint

$$x\tilde{x} = \frac{1 + \tau}{4\gamma^2}. \quad (2.25)$$

In this notation

$$-q_1^2 = \mathbf{q}_{1\perp}^2 + (2m_e x)^2, \quad -q_2^2 = \mathbf{q}_{2\perp}^2 + (2m_e \tilde{x})^2. \quad (2.26)$$

It is useful to note that the rapidity of the Ps is equal to $(1/2) \ln(x/\tilde{x})$ and that the variables x and \tilde{x} have a very simple form for relativistic Ps. Indeed, for $p_z \gg m_e$ the variable x is $x = \varepsilon/(2m_e\gamma)$, i.e. x is the ratio of Ps energy to the characteristic energy $2m_e\gamma$ (above $2m_e\gamma$ the spectrum drops very quickly). Analogously, for $(-p_z) \gg m_e$ $\tilde{x} = \varepsilon/(2m_e\gamma)$. The neglected contributions are of the order of $(4m_e^2 + \mathbf{p}_\perp^2)/\varepsilon^2$. From the discussion in Sect. II B it follows that the dominant contribution to the cross i section (2.23) is given by the region

$$\frac{1}{\gamma^2} \lesssim x, \quad \tilde{x} \lesssim 1, \quad x^2 + \tilde{x}^2 \lesssim \tau \lesssim 1. \quad (2.27)$$

In Appendix B we show that the function J_B can be reduced to the one-dimensional integral

$$J_B = \frac{\tau}{8} \int_0^1 u^3 (1-u)(2-u)^2 K(u, x, \tau) du, \quad (2.28)$$

$$K(u, x, \tau) = 3 \int_{-1}^1 \frac{(1-t^2) dt}{(at^2 + bt + c)^4} \quad (2.29)$$

$$= \frac{12a(b^2 - 5a^2 + ac)}{d^{7/2}} \ln \frac{c - a + \sqrt{d}}{c - a - \sqrt{d}} + \frac{4N}{[(a+c)^2 - b^2]^2 d^3},$$

$$N = -30a^6 + b^6 - 104a^5c + 56a^4b^2 - 124a^4c^2 + 90a^3b^2c - 56a^3c^3$$

$$- 26a^2b^4 + 36a^2b^2c^2 - 6a^2c^4 - 2ab^4c - 6ab^2c^3$$

where

$$a = -\frac{1}{4}u^2\tau, \quad b = \frac{1}{2}u(2-u)(x^2 - \tilde{x}^2),$$

$$c = \frac{1}{4}(2-u)^2\tau + \frac{1}{2}(2-u)^2(x^2 + \tilde{x}^2) + (1-u)(2-u), \quad d = b^2 - 4ac. \quad (2.30)$$

Let us stress that the inclusive cross section (2.23) with (2.28) is valid both for relativistic para-Ps with $\varepsilon \gg 2m_e$ as well and for nonrelativistic para-Ps with $\varepsilon \sim 2m_e$.

Using the representation (2.23) for J_B it is not difficult to find that the inclusive cross section is large in the main region

$$J_B = \frac{1}{\tau} \left[\ln(4\gamma^2\tau) - 1 \right] \quad \text{at} \quad x^2 + \tilde{x}^2 \ll \tau \ll 1 \quad (2.31)$$

but drops very quickly outside this region. Indeed, the function J_B is small at large τ

$$J_B = \frac{1}{\tau^3} \ln(4\gamma^2) \quad \text{at} \quad x^2 + \tilde{x}^2 \ll 1 \ll \tau, \quad (2.32)$$

at large x

$$J_B = \frac{\tau}{x^8} \ln(4\gamma^2 x^2) \quad \text{at} \quad \tau \ll 1 \ll x^2, \quad (2.33)$$

and at very small τ

$$J_B = \frac{\tau}{(x^2 - \tilde{x}^2)^2} \left(\frac{x^2 + \tilde{x}^2}{x^2 - \tilde{x}^2} \ln \frac{x}{\tilde{x}} - 1 \right) \quad \text{at} \quad \tau \ll x^2 + \tilde{x}^2 \ll 1. \quad (2.34)$$

In Figs. 2,3 we present the inclusive cross section (2.23) at the RHIC and the LHC (Pb–Pb mode) as function of the scaled Ps energy for different scaled transverse momenta squared τ . From these Figures it is obvious that for $\varepsilon < \sqrt{\tau}$ the cross sections only weakly depend on the Ps energy. The cross sections quickly drop at larger energies.

To obtain the **spectrum** of relativistic Ps it is convenient to use an approach developed in Ref. [11] for the electroproduction of Ps on nucleus $eA \rightarrow eA + \text{Ps}$ (Fig. 4). It is well known that the electroproduction cross section can be exactly written in terms of two structure functions or two cross section $\sigma_T(s_\gamma, q^2)$ and $\sigma_S(s_\gamma, q^2)$ for the virtual processes $\gamma_T^* A \rightarrow \text{Ps} + A$ and $\gamma_S^* A \rightarrow \text{Ps} + A$ (where γ_T^* and γ_S^* denote the transverse and scalar virtual photons with 4-momentum q and helicity $\lambda_T = \pm 1$ and $\lambda_S = 0$, respectively, and $s_\gamma = 2qP_2$):

$$d\sigma(eA \rightarrow \text{Ps} + A) = \sigma_T(s_\gamma, q^2) dn_T(s_\gamma, q^2) + \sigma_S(s_\gamma, q^2) dn_S(s_\gamma, q^2). \quad (2.35)$$

Here the coefficients dn_T and dn_S can be called the number of the transverse and scalar photons generated by the electron.

To calculate $d\sigma_B$ in our case we can use a similar expression where the number of photons are now generated from a scalar projectile nucleus. The cross sections σ_T and σ_S for para-Ps have been obtained in Ref. [11] for high energetic virtual photons (for $s_\gamma \gg 4m_e M$ or $\gamma^2 x \gg 1$):

$$\sigma_T = \pi\zeta(3) \frac{Z^2\alpha^6}{m_e^2} \frac{L(x, y) - 1}{(1+y)^2}, \quad \sigma_S = 0 \quad (2.36)$$

with

$$L(x, y) = \ln(4\gamma^2 x) - \frac{1}{2} \ln(1+y), \quad y = \frac{-q_1^2}{4m_e^2}. \quad (2.37)$$

Here x is defined in Eq. (2.24). The accuracy of Eq. (2.36) is determined by neglecting terms $\sim 1/(\gamma^2 x)$, $\sqrt{-q_1^2}/(m_e \gamma^2 x)$. The number of photons generated by the first nucleus are (see, for example Appendix D from Ref. [14])

$$dn_T = \frac{Z^2 \alpha}{\pi} \left(1 - \frac{x^2}{y}\right) \frac{dx}{x} \frac{dy}{y},$$

$$dn_S = \frac{Z^2 \alpha}{\pi} \frac{dx}{x} \frac{dy}{y}. \quad (2.38)$$

Note that dn_T corresponds to dn_1 as given in Eq. (2.10).

Using Eqs. (2.36)-(2.38) and integrating over y we obtain²

$$d\sigma_B = \zeta(3) \sigma_0 \left\{ f_1(x) \left[\ln(4\gamma^2 x) - 1 \right] - f_2(x) \right\} \frac{dx}{x} \quad (2.39)$$

with

$$f_1(x) = \int_{x^2}^{\infty} \left(1 - \frac{x^2}{y}\right) \frac{dy}{y(1+y)^2} = (1 + 2x^2) \ln \frac{1+x^2}{x^2} - 2,$$

$$f_2(x) = \frac{1}{2} \int_{x^2}^{\infty} \left(1 - \frac{x^2}{y}\right) \frac{\ln(1+y)}{y} \frac{dy}{(1+y)^2} \quad (2.40)$$

$$= \frac{1+2x^2}{2} \left[\frac{\pi^2}{6} - \text{Li}_2\left(\frac{x^2}{1+x^2}\right) \right] - \frac{1}{2} x^2 \ln \frac{1+x^2}{x^2} - \frac{1}{2} - \ln(1+x^2).$$

Here the dilogarithmic function is defined as

$$\text{Li}_2(x) = - \int_0^x \frac{\ln(1-t)}{t} dt. \quad (2.41)$$

For small $x \ll 1$ we have

$$f_1(x) = 2 \left(\ln \frac{1}{x} - 1 \right), \quad f_2(0) = \frac{\pi^2 - 6}{12} = 0.3225 \quad (2.42)$$

while for large $x \gg 1$

$$f_1(x) = \frac{1}{6x^4}, \quad f_2(x) = \frac{1}{6x^4} \left(\ln x + \frac{5}{12} \right). \quad (2.43)$$

In obtaining Eq. (2.39), we have considered the first nucleus as projectile and the second nucleus as target. Taking the first nucleus as target and the second nucleus as projectile we find for $d\sigma_B$ the same expression as in Eq. (2.39) with the replacement $x \rightarrow \tilde{x}$:

$$d\sigma_B = \zeta(3) \sigma_0 \left\{ f_1(\tilde{x}) \left[\ln(4\gamma^2 \tilde{x}) - 1 \right] - f_2(\tilde{x}) \right\} \frac{d\tilde{x}}{\tilde{x}}. \quad (2.44)$$

²The lower limit is $y_{min} = x^2$, the upper limit can be extended to infinity due to the fast convergence of the integral.

To obtain the spectrum $d\sigma_B/d\varepsilon$ we have to take into account the following two circumstances for the relativistic Ps: i (i) the variables x and \tilde{x} are related in a simple way to ε ; (ii) there are two symmetrical regions in the c.m.s.: $p_z \approx \varepsilon \gg 2m_e$ and $(-p_z) \approx \varepsilon \gg 2m_e$. In the first region the variable x is $x = \varepsilon/(2m_e\gamma)$ and we have to use Eq. (2.39), in the second region $\tilde{x} = \varepsilon/(2m_e\gamma)$ where Eq. (2.44) is used. As a result, the spectrum for the relativistic Ps has the form (compare with the approximate Eq. (2.18))

$$d\sigma_B = 2\zeta(3) \sigma_0 \left[f_1 \left(\frac{\varepsilon}{2m_e\gamma} \right) \left(\ln \frac{2\varepsilon\gamma}{m_e} - 1 \right) - f_2 \left(\frac{\varepsilon}{2m_e\gamma} \right) \right] \frac{d\varepsilon}{\varepsilon}. \quad (2.45)$$

The accuracy of this expression is determined by the omitted terms of the order of $1/\gamma^2$, $2m_e/(\varepsilon\gamma)$, $(2m_e/\varepsilon)^2$.

Note that in the main region $2m_e \ll \varepsilon \ll 2m_e\gamma$ the spectrum is logarithmically enhanced

$$d\sigma_B = 4\zeta(3) \sigma_0 \left[\ln \frac{2m_e\gamma}{\varepsilon} \ln \frac{2\varepsilon\gamma}{m_e} - \ln(4\gamma^2) + \frac{30 - \pi^2}{24} \right] \frac{d\varepsilon}{\varepsilon} \quad (2.46)$$

while for large $\varepsilon \gg 2m_e\gamma$ the spectrum drops very quickly

$$d\sigma_B = \frac{\zeta(3)}{3} \sigma_0 \left(\frac{2m_e\gamma}{\varepsilon} \right)^4 \left[\ln(4\gamma^2) - \frac{17}{12} \right] \frac{d\varepsilon}{\varepsilon}. \quad (2.47)$$

The spectrum of the para-Ps is shown in Fig. 5. The solid and dash-dotted lines present the result for the RHIC and the LHC (Pb–Pb mode) obtained by a numerical integration of the inclusive cross section (2.23), (2.28). The dashed and dotted lines present the spectrum for both colliders calculated from Eq. (2.45) which is valid for relativistic Ps with $\varepsilon \gg 2m_e$. It can be seen that in the region $10m_e < \varepsilon < (0.1 \div 0.2) 2m_e\gamma$ the quantity $\varepsilon d\sigma_B/d\varepsilon$ has a very weak dependence on ε whereas the spectra drop quickly for $\varepsilon/(2m_e\gamma) \gtrsim 0.5$.

From the experimental point of view, it is interesting to integrate the cross section over the region $\varepsilon \geq \varepsilon_{\min}$ (where $2m_e \ll \varepsilon_{\min} \ll 2m_e\gamma$). It can be obtained from Eq. (2.45) omitting pieces of the order of $\varepsilon_{\min}^2/[(2m_e\gamma)^2 l]$:

$$\sigma_B = 2\zeta(3) \sigma_0 \left[\ln(4\gamma^2) \left(l^2 - 2l + \frac{\pi^2 + 12}{12} \right) - \frac{2}{3}l^3 + \frac{30 - \pi^2}{12}l - c \right], \quad (2.48)$$

where

$$c = \frac{\pi^2 + 3\zeta(3) + 21}{12} = 2.873, \quad l = \ln \frac{2m_e\gamma}{\varepsilon_{\min}}.$$

Using this expression for $\varepsilon_{\min} = 15m_e$ and the results of a numerical integration in the region $2m_e < \varepsilon < 15m_e$, we obtain the total cross section for the Born contribution:

$$\sigma_B = 17.8 \text{ mb for RHIC}, \quad 110 \text{ mb for LHC (Pb–Pb)}, \quad 0.42 \text{ mb for LHC (Ca–Ca)}. \quad (2.49)$$

D. An approximate calculation of the Coulomb correction

Let us consider the correction $d\sigma_1$ defined in Eq. (2.2). Its contribution to the spectrum can be calculated just by the same method as it was done for the Born contribution. According to Ref. [11] we have to replace in Eq. (2.36)

$$L(x, y) - 1 \rightarrow -C(\nu) \quad (2.50)$$

from which it follows

$$d\sigma_1 = -\zeta(3) \sigma_0 C(\nu) f_1(x) \frac{dx}{x}. \quad (2.51)$$

The quantity $C(\nu)$ is defined with the help of function $F(a, b; c; z)$ — the Gauss hypergeometric function:

$$C(\nu) = \int_0^\infty F(\tau, \nu) d\tau, \quad z = \left(\frac{1-\tau}{1+\tau} \right)^2, \quad (2.52)$$

$$F(\tau, \nu) = \frac{1}{2\tau(1+\tau)^2} \left\{ 1 - \left[F(i\nu, -i\nu; 1; z) \frac{\pi\nu}{\sinh \pi\nu} \right]^2 \right\}.$$

The curve $C(\nu)$ and properties of the function $F(\tau, \nu)$ are given in [11], we mention here only that $C(\nu) = 0.6734$ for Au, 0.7080 for Pb and

$$C(\nu) = 2.9798 \nu^2 \quad \text{at} \quad \nu^2 \ll 1. \quad (2.53)$$

Analogously,

$$d\tilde{\sigma}_1 = -\zeta(3) \sigma_0 C(\nu) f_1(\tilde{x}) \frac{d\tilde{x}}{\tilde{x}}. \quad (2.54)$$

As we have explained in Sect. II A, the spectra $d\sigma_1/d\varepsilon$ and $d\tilde{\sigma}_1/d\varepsilon$ have to be calculated with logarithmic accuracy only. Within this accuracy we have $x \approx \omega_1/(2m_e\gamma)$ and $\tilde{x} \approx \omega_2/(2m_e\gamma)$. Then for $d\sigma_1$ we can repeat the calculations similar to those which we have already performed to get the spectrum (2.18) from expression (2.14). In our case this gives

$$d\sigma_1 = -2\zeta(3) \sigma_0 C(\nu) \ln \gamma^2 \frac{d\varepsilon}{\varepsilon}, \quad 2m_e \ll \varepsilon \ll 2m_e\gamma. \quad (2.55)$$

Taking into account the same contribution from $d\tilde{\sigma}_1$ we find (with logarithmic accuracy)

$$d(\sigma_1 + \tilde{\sigma}_1) = -4\zeta(3) \sigma_0 C(\nu) \ln \gamma^2 \frac{d\varepsilon}{\varepsilon}, \quad 2m_e \ll \varepsilon \ll 2m_e\gamma. \quad (2.56)$$

The total contribution of CC to the para-Ps production is

$$\sigma_{\text{para}}^{\text{CC}} = \sigma_1 + \tilde{\sigma}_1 = -2\zeta(3) \sigma_0 C(\nu) [\ln \gamma^2]^2 \quad (2.57)$$

from which it follow that the relative contribution of CC is

$$\frac{\sigma_{\text{para}}^{\text{CC}}}{\sigma_{\text{para}}^{\text{LLA}}} \approx -\frac{6C(\nu)}{\ln \gamma^2}, \quad (2.58)$$

i.e. it is -43% for RHIC, -27% for LHC (Pb–Pb) and -2.2% for LHC (Ca–Ca).

To obtain the contribution of $d\sigma_1$ to the inclusive cross section we can explore Eq. (2.52). Strictly speaking, the variable τ in that equation is $\tau = \mathbf{p}_\perp^2/(4m_e^2 - q_1^2)$. But in LLA used here for $d\sigma_1$ we can take the function $F(\tau, \nu)$ on the mass shell of the first virtual photon (at $q_1^2 = 0$), i.e. we can use $\tau = \mathbf{p}_\perp^2/(4m_e^2)$. Now with the help of a simple relation

$$\frac{dx}{x} d\tau = \frac{1}{4\pi m_e^2} \frac{d^3p}{\varepsilon} \quad (2.59)$$

we obtain

$$\varepsilon \frac{d^3\sigma_1}{d^3p} = \frac{\zeta(3)}{4\pi} \frac{\sigma_0}{m_e^2} J_1, \quad J_1 = -f_1(x) F(\tau, \nu). \quad (2.60)$$

Analogously, for $d\tilde{\sigma}_1$ we find

$$\tilde{J}_1 = -f_1(\tilde{x}) F(\tau, \nu). \quad (2.61)$$

The function $f_1(x)$ is defined in (2.40). As a result, the inclusive cross section reads

$$\varepsilon \frac{d^3\sigma_{\text{para}}}{d^3p} = \frac{\zeta(3)}{4\pi} \frac{\sigma_0}{m_e^2} J_{\text{para}}, \quad J_{\text{para}} = J_{\text{B}} - [f_1(x) + f_1(\tilde{x})] F(\tau, \nu) \quad (2.62)$$

where J_{B} is defined in (2.28), x and \tilde{x} are defined in Eqs. (2.24). In the LLA we have

$$f_1(x) + f_1(\tilde{x}) = 2 \ln \gamma^2, \quad 2m_e \ll \varepsilon \ll 2m_e \gamma. \quad (2.63)$$

III. THE PRODUCTION OF ORTHO–PS

The amplitude of the ortho–Ps production can be presented in the form (compare with Eq. (2.1))

$$M_{\text{ortho}} = M_1 + \tilde{M}_1 + M_2, \quad (3.1)$$

$$M_1 = \sum_{n'=2,4,6,\dots} M_{1n'}, \quad \tilde{M}_1 = \sum_{n=2,4,6,\dots} M_{n1}, \quad M_2 = \sum_{n,n'\geq 2} M_{nn'}.$$

with sum $n + n'$ being odd. The total cross section reads (compare with Eq. (2.2))

$$\sigma_{\text{ortho}} = \sigma_1 + \tilde{\sigma}_1 + \sigma_2, \quad d\sigma_1 \propto |M_1|^2, \quad d\tilde{\sigma}_1 \propto |\tilde{M}_1|^2, \quad (3.2)$$

$$d\sigma_2 \propto 2\text{Re}(M_1 \tilde{M}_1^* + M_1 M_2^* + \tilde{M}_1 M_2^*) + |M_2|^2.$$

Since $\text{Re}(M_1 \tilde{M}_1^*)$ disappears after azimuthal averaging, it is not difficult to estimate that

$$\frac{\sigma_2}{\sigma_1} \sim \frac{\nu^2}{\ln \gamma^2} < 4\% \quad (3.3)$$

for the colliders in Table I. Therefore,

$$\sigma_{\text{ortho}} = \sigma_1 + \tilde{\sigma}_1 \quad (3.4)$$

with an accuracy of the order of 4 %; moreover, with the same accuracy we can calculate σ_1 and $\tilde{\sigma}_1$ in LLA only.

To obtain the **inclusive cross section** we use the relation (2.35) with dn_T and dn_S from Eqs. (2.38) and the cross sections $d\sigma_T$ and $d\sigma_S$ for ortho-Ps from Eqs. (3.22) of Ref. [11]

$$\begin{aligned} d\sigma_T &= 4\pi\zeta(3) \frac{Z^4\alpha^8}{m_e^2} \Phi_t^2(\tau, \nu) \frac{d\tau}{(1+y)^3}, \quad d\sigma_S = y d\sigma_T, \\ \Phi_t(\tau, \nu) &= \frac{1-\tau}{(1+\tau)^3} F(1+i\nu, 1-i\nu; 2; z) \frac{\pi\nu}{\sinh \pi\nu} \end{aligned} \quad (3.5)$$

where z is defined in Eq. (2.52).

It gives

$$\varepsilon \frac{d^3\sigma_{\text{ortho}}}{d^3p} = \frac{\zeta(3)}{\pi} \frac{\nu^2\sigma_0}{m_e^2} \Phi_t^2(\tau, \nu) [f_3(x) + f_3(\tilde{x})], \quad (3.6)$$

$$f_3(x) = \int_{x^2}^{\infty} \left(1 - \frac{x^2}{y} + y\right) \frac{dy}{y(1+y)^3} = (1+3x^2) \ln \frac{1+x^2}{x^2} - 2 - x^2 \frac{3+2x^2}{2(1+x^2)^2}.$$

The properties of the function $\Phi_t^2(\tau, \nu)$, which determines the angular distribution of the produced ortho-Ps, are described in Ref. [11]. We mention here only that the typical values of τ are $\tau \sim 0.1$ which correspond to a characteristic emission angle of ortho-Ps

$$\theta \sim \frac{m_e}{\varepsilon}. \quad (3.7)$$

The function $f_3(x)$ is large at small values of x

$$f_3(x) = 2 \left(\ln \frac{1}{x} - 1 \right) \quad \text{at } x \ll 1 \quad (3.8)$$

and small at large x

$$f_3(x) = \frac{1}{2x^4} \quad \text{at } x \gg 1.$$

In the LLA we have

$$f_3(x) + f_3(\tilde{x}) \approx 2 \ln \gamma^2, \quad 2m_e \ll \varepsilon \ll 2m_e\gamma. \quad (3.9)$$

For the **spectrum** of ortho-Ps in the LLA we obtain the expression

$$d\sigma_{\text{ortho}} = 16\zeta(3) \nu^2\sigma_0 B(\nu) \ln \gamma^2 \frac{d\varepsilon}{\varepsilon}, \quad B(\nu) = \int_0^{\infty} \Phi_t^2(\tau, \nu) d\tau. \quad (3.10)$$

Note that $B(\nu) = 0.3770$ for Au, 0.3654 for Pb and

$$B(\nu) = 0.6137 - 1.7073\nu^2 \quad \text{at } \nu \ll 1. \quad (3.11)$$

After integrating the spectrum (3.10) over ε in the region $2m_e \lesssim \varepsilon \lesssim 2m_e\gamma$ we obtain the total cross section in the LLA

$$\sigma_{\text{ortho}} = 8\zeta(3) \nu^2 \sigma_0 B(\nu) [\ln \gamma^2]^2 . \quad (3.12)$$

The ortho-Ps production in lowest order in $Z\alpha$ (production via three photons) is described by Eq. (3.12) with $B(0) = 2 - 2 \ln 2 = 0.6137$. Therefore, the relative order of the Coulomb correction (corresponding to the production with 5, 7, 9, ... photons) is given by ratio

$$\frac{B(\nu) - B(0)}{B(0)} . \quad (3.13)$$

This ratio is equal to -39% for the RHIC, for the LHC is reaches -40% in the Pb-Pb mode and -3.6% in the Ca-Ca mode.

IV. DISCUSSION

1. We have calculated the cross sections for the production of parapositronium (omitting terms $\sim (Z\alpha)^2/L^2 < 0.4\%$, $L = \ln \gamma^2$) and orthopositronium (omitting contributions $\sim (Z\alpha)^2/L < 4\%$) at the RHIC and the LHC. Our results are summarized in Table II. From that Table we observe that the production rate is well above 10^5 events per day, therefore measurements will be possible with a high precision at these colliders. We note that the production rate for the long living ortho-Ps is also relatively high, irrespectively of the suppression factor $(Z\alpha)^2$.

2. In these calculations we take into account not only the lowest order in the parameter $Z\alpha$ but the whole series in $Z\alpha$ — the so called Coulomb correction. They decrease the total cross section for the para-Ps production by about 30 % and 50 % for Au-Au and Pb-Pb collisions and by about 40 % for ortho-Ps production in the same collisions. For Ca-Ca collisions the CC are small $\sim 3\%$.

3. We have presented the inclusive cross sections (see Eqs. (2.23), (2.28), (2.62), (3.6) and Figs. 2,3) and the spectra for the Ps production (see Eqs. (2.45), (2.56), (3.10) and Fig. 5). From these results we conclude that the number of relativistic Ps with a Lorentz factors up to the Lorentz factor of the ion γ will be large enough to be detected.

4. The signature of the events is quite clear: the colliding ions practically do not change their motion and after the collision they remain in their bunches. In the central detector no hadrons should be observed. The further separation of the relativistic Ps from the background can be performed using a method tested in a Serpukhov experiment (see Ref [15]). In that experiment a special channel with a vacuum pipe of about 40 m length was used and a weak transverse magnetic field inside this pipe eliminates the charged particles. At the end of the pipe a strong magnetic field forces the Ps to break into e^+ and e^- which are easily detectable.

ACKNOWLEDGMENTS

We are grateful to I. Ginzburg, I. Khriplovich and I. Meshkov for useful discussions. We are indebted to S. Klein and L. Nemenov for clarifying the experimental situation. The work of E.A.K. was supported by INTAS grant 93-239 ext, the work of G.L.K and V.G.S is

supported by Volkswagen Stiftung (Az. No.I/72 302) and by Russian Foundation for Basic Research (grant 96-02-19114).

APPENDIX A: THE BORN AMPLITUDE FOR THE PARA-PS PRODUCTION

It is useful to introduce the “almost light-like” 4-vectors

$$\tilde{P}_1 = P_1 - \frac{M^2}{s}P_2, \quad \tilde{P}_2 = P_2 - \frac{M^2}{s}P_1, \quad \tilde{P}_i^2 = \frac{M^6}{s^2}, \quad s = 2P_1P_2 \approx 2\tilde{P}_1\tilde{P}_2 \gg M^2$$

and to decompose the 4-vectors q_i into components in the plane of the 4-vectors \tilde{P}_1 and \tilde{P}_2 and in the plane orthogonal to them

$$q_i = \alpha_i\tilde{P}_2 + \beta_i\tilde{P}_1 + q_{i\perp}, \quad \alpha_i = \frac{2q_i\tilde{P}_1}{s}, \quad \beta_i = \frac{2q_i\tilde{P}_2}{s}. \quad (\text{A1})$$

The quantities α_i and β_i are the so called Sudakov variables. It is not difficult to estimate that

$$\frac{|\alpha_1|}{\beta_1} \approx \frac{|q_1^2|}{2q_1P_2} < \frac{|q_1^2|}{4m_eM} \ll 1, \quad \frac{|\beta_2|}{\alpha_2} \approx \frac{|q_2^2|}{2q_2P_1} < \frac{|q_2^2|}{4m_eM} \ll 1. \quad (\text{A2})$$

In the used c.m.s. the 4-vectors $q_{i\perp}$ have x and y components only

$$q_{i\perp} = (0, q_{ix}, q_{iy}, 0) = (0, \mathbf{q}_{i\perp}, 0), \quad q_{i\perp}^2 = -\mathbf{q}_{i\perp}^2.$$

The relativistic nuclei in the Ps production can be regarded as point-like and spinless particles. Therefore, the Born amplitude has the form (see Fig. 1 for the notations)

$$M_B = 4\pi Z^2 \alpha \frac{(P_1 + P_1')^\mu (P_2 + P_2')^\nu}{q_1^2 q_2^2} M_{\mu\nu}$$

where $M_{\mu\nu}$ is the amplitude for the virtual process $\gamma^*\gamma^* \rightarrow \text{Ps}$. Due to gauge invariance we have

$$q_1^\mu M_{\mu\nu} = (\alpha_1\tilde{P}_2 + \beta_1\tilde{P}_1 + q_{1\perp})^\mu M_{\mu\nu} = 0.$$

This expression can be transformed to (using the estimates (A2))

$$(P_1 + P_1')^\mu M_{\mu\nu} = 2P_1^\mu M_{\mu\nu} \approx -\frac{2q_{1\perp}^\mu}{\beta_1} M_{\mu\nu}.$$

Analogously we find

$$(P_2 + P_2')^\nu M_{\mu\nu} \approx -\frac{2q_{2\perp}^\nu}{\alpha_2} M_{\mu\nu}$$

which leads to the result

$$M_B = \frac{16\pi Z^2 \alpha}{\beta_1 \alpha_2} \frac{q_{1\perp}^\mu q_{2\perp}^\nu}{q_1^2 q_2^2} M_{\mu\nu}. \quad (\text{A3})$$

Using the rules (2.11) from Ref. [11] for the transition from the pair production $AA \rightarrow AAe^+e^-$ to the process $AA \rightarrow AA + \text{Ps}$, we obtain the Born amplitude for the production of the para-positronium in the quantum state n^1S_0

$$M_B = \frac{4(4\pi Z\alpha)^2 m_e \alpha^{3/2}}{\beta_1 \alpha_2 q_1^2 q_2^2 \sqrt{4\pi n^3}} \times \frac{1}{4} \text{Tr} \left\{ \left[\hat{q}_{1\perp} \frac{\hat{p}_- - \hat{q}_1 + m_e}{(p_- - q_1)^2 - m_e^2} \hat{q}_{2\perp} + \hat{q}_{2\perp} \frac{\hat{p}_- - \hat{q}_2 + m_e}{(p_- - q_2)^2 - m_e^2} \hat{q}_{1\perp} \right] (\hat{p} + m_{Ps}) i\gamma^5 \right\}$$

where $p_+ = p_- = p/2$. Taking the trace and using the estimates (A2) we obtain

$$M_B = -16Z^2 \sqrt{\frac{\pi^3 \alpha^7}{n^3}} \frac{s}{m_e} \frac{(\mathbf{q}_{1\perp} \times \mathbf{q}_{2\perp}) \cdot \mathbf{n}_1}{q_1^2 q_2^2} \frac{4m_e^2}{4m_e^2 - q_1^2 - q_2^2}, \quad (\text{A4})$$

$$\mathbf{n}_1 = \frac{\mathbf{P}_1}{|\mathbf{P}_1|}.$$

From that Born amplitude we find the inclusive cross section for the production of para-Ps summed over quantum states n

$$\varepsilon \frac{d^3 \sigma_B}{d^3 p} = \frac{1}{8(2\pi)^5 s^2} \sum_{n=1}^{\infty} \int |M_B|^2 \delta(\mathbf{q}_{1\perp} + \mathbf{q}_{2\perp} - \mathbf{p}_\perp) d^2 q_{1\perp} d^2 q_{2\perp}. \quad (\text{A5})$$

Now we derive a useful expression for the virtualities q_i^2 . From the obvious relations $(P_1 - q_1)^2 = M^2$ or $2q_1 P_1 = s\alpha_1 + M^2\beta_1 = q_1^2 = s\alpha_1\beta_1 + q_{1\perp}^2$ and $2q_2 P_1 = s\beta_2 + M^2\alpha_2 = q_2^2 = s\alpha_2\beta_2 + q_{2\perp}^2$ we obtain

$$q_1^2 = \frac{q_{1\perp}^2 - (M\beta_1)^2}{1 - \beta_1}, \quad q_2^2 = \frac{q_{2\perp}^2 - (M\alpha_2)^2}{1 - \alpha_2}. \quad (\text{A6})$$

Further, from the relation $(q_1 + q_2)^2 = p^2 = 4m_e^2$ we get (using the inequalities (A2))

$$s\alpha_2\beta_1 + p_\perp^2 = 4m_e^2. \quad (\text{A7})$$

If we introduce variables $x = M\beta_1/(2m_e)$ and $\tilde{x} = M\alpha_2/(2m_e)$ we immediately obtain from Eqs. (A6)-(A7) and inequalities (2.7) the expressions (2.24)-(2.26).

APPENDIX B: CALCULATION OF J_B FROM EQ. (2.23)

Let us introduce the two-dimensional vectors $\mathbf{k}_i = \mathbf{q}_{i\perp}/(2m_e)$ and the quantities $V_1 = \mathbf{k}_1^2 + x^2$, $V_2 = \mathbf{k}_2^2 + \tilde{x}^2$, $V_3 = V_1 + V_2 + 1$. Then the integral J_B from Eq. (2.23) transforms to

$$J_B = \frac{1}{\pi} \int \frac{(\mathbf{k}_1 \times \mathbf{k}_2)^2}{(V_1 V_2 V_3)^2} \delta\left(\mathbf{k}_1 + \mathbf{k}_2 - \frac{\mathbf{P}_\perp}{2m_e}\right) d^2 k_1 d^2 k_2. \quad (\text{B1})$$

Now we use the usual Feynman trick

$$\frac{1}{(V_1 V_2 V_3)^2} = 5! \int \frac{\delta(\sum_j \alpha_j - 1) \prod_j \alpha_j d\alpha_j}{(\sum_j \alpha_j V_j)^6}$$

and perform the integration over \mathbf{k}_i :

$$J_B = 3\tau \int_0^1 d\alpha_1 \int_0^{1-\alpha_1} d\alpha_2 \frac{\alpha_1 \alpha_2 (1 - \alpha_1 - \alpha_2) (2 - \alpha_1 - \alpha_2)^2}{D^4}, \quad (\text{B2})$$

$$D = (1 - \alpha_1)(1 - \alpha_2)\tau + (2 - \alpha_1 - \alpha_2)[1 - \alpha_1 - \alpha_2 + (1 - \alpha_2)x^2 + (1 - \alpha_1)\tilde{x}^2]$$

where τ is given in Eq. (2.24). Substituting

$$2\alpha_1 = (1 + t)u, \quad 2\alpha_2 = (1 - t)u$$

we present Eq. (B2) in the form

$$J_B = \frac{3}{8} \tau \int_0^1 du u^3 (1 - u) (2 - u)^2 \int_{-1}^1 dt \frac{(1 - t^2)}{D^4}, \quad (\text{B3})$$

$$D = \tau \left[1 - u + \frac{1}{4}u^2(1 - t^2) \right] + (2 - u) \left[1 - u + x^2 + \tilde{x}^2 - \frac{1}{2}u(1 - t)x^2 - \frac{1}{2}u(1 + t)\tilde{x}^2 \right]$$

which is equivalent to Eqs. (2.28)-(2.30).

REFERENCES

- [1] I. N. Meshkov, *Elem. Particles and Nuclei* **28**, 495 (1997).
- [2] I. B. Khriplovich, A. I. Milstein, Novosibirsk Budker Institute preprint Budker-INP 96-49 (1996); I. B. Khriplovich, I. N. Meshkov, A. I. Milstein, *JINR Rapid Comm. No 3(83)-97*, 68 (1997).
- [3] L. L. Nemenov, JINR Dubna preprint P2-81-263 (1981); *Yad. Fiz.* **39**, 1306 (1981); *Yad. Fiz.* **51**, 444 (1990) [*Sov. J. Nucl. Phys.* **51** 284 (1990)];
- [4] V. L. Lyuboshitz, M. I. Podgoretsky, *ZhETF* **81**, 1556 (1981).
- [5] G. V. Meledin, V. G. Serbo, A. K. Slivkov, *Pis'ma ZhETF* **13**, 98 (1971) [*JETP Lett.* **13**, 68 (1971)].
- [6] H. A. Olsen, *Phys. Rev. D* **33**, 2033 (1986).
- [7] V. L. Lyuboshitz, *Yad. Fiz.* **45**, 1099 (1987).
- [8] A. V. Tarasov, I. V. Christova, JINR Dubna preprint P2-91-4, (1991).
- [9] A. A. Akhundov, D. Yu. Bardin, L. L. Nemenov, *Yad. Fiz.* **27**, 1542 (1978).
- [10] E. Holvik, H. A. Olsen, *Phys. Rev. D* **35**, 2124 (1987).
- [11] S. R. Gevorkyan, E. A. Kuraev, A. Schiller, V. G. Serbo, A. B. Tarasov, *Phys. Rev. A* **58** 4556 (1998).
- [12] I. N. Meshkov, A. N. Skrinsky, *Nucl. Instrum. Meth., A* **379**, 41 (1996).
- [13] C. Caso et al., *Eur. Phys. J. C* **3**, 1 (1998); S. Klein (private communication).
- [14] V. M. Budnev, I. F. Ginzburg, G. V. Meledin, V. G. Serbo, *Phys. Rep. C* **15**, 181 (1975).
- [15] G. D. Alekseev et al. *Yad. Fiz.* **40**, 139 (1984).

TABLES

<i>Collider, mode</i>	<i>Lorentz factor</i> $\gamma = E/M$	<i>Luminosity</i> $\mathcal{L}, \text{cm}^2\text{s}^{-1}$
RHIC, Au–Au	108	$2 \cdot 10^{26}$
LHC, Pb–Pb	3000	$2 \cdot 10^{27}$
LHC, Ca–Ca	3750	$4 \cdot 10^{30}$

TABLE I. Parameters of the discussed colliders.

<i>Collider, mode</i>	σ_{para} mb	para–Ps events/sec	σ_{ortho} mb	ortho–Ps events/sec
RHIC, Au–Au	8.7	1.7	6.8	1.4
LHC, Pb–Pb	78	155	24	48
LHC, Ca–Ca	0.41	1650	0.0086	35

TABLE II. Cross sections and event rates at the RHIC and LHC.

FIGURES

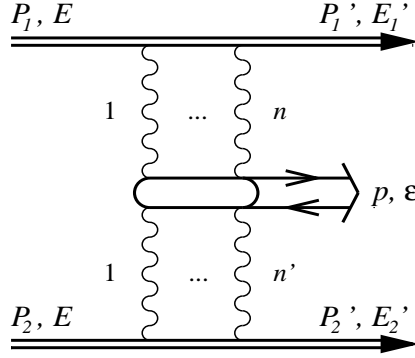


FIG. 1. The amplitude $M_{nn'}$ for the production of Ps by n (n') virtual photons emitted by the first (second) nucleus.

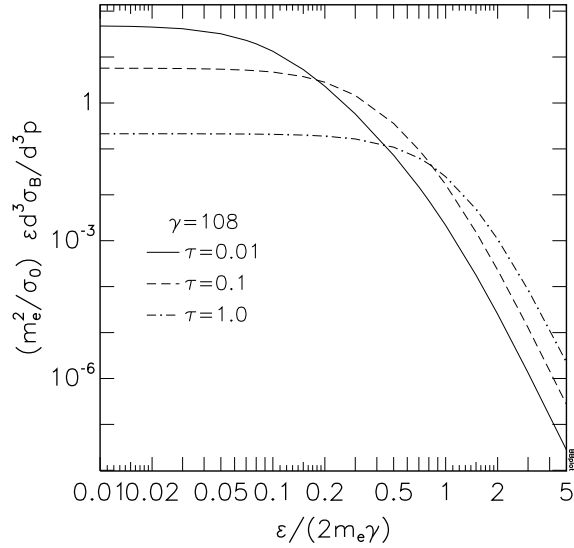


FIG. 2. The inclusive cross section (2.23) as function of the scaled para-Ps energy $\varepsilon/(2m_e\gamma)$ for the RHIC at different values of $\tau = \mathbf{p}_\perp^2/(2m_e)^2$.

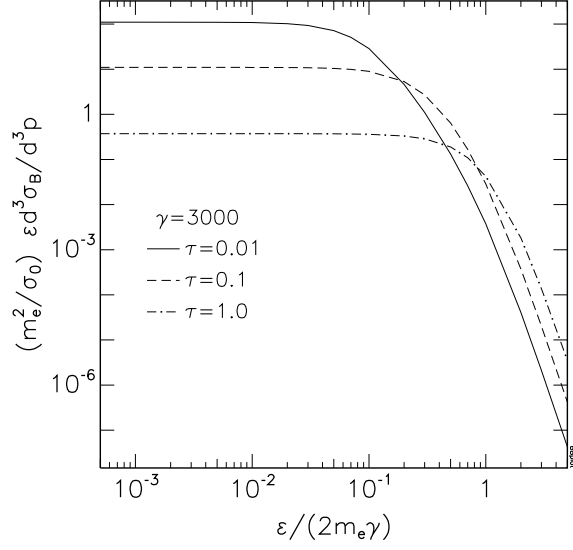


FIG. 3. Same as Fig. 2 for the LHC (Pb-Pb mode)

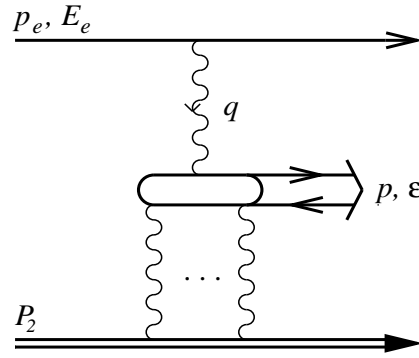


FIG. 4. The electroproduction of Ps on a nucleus.

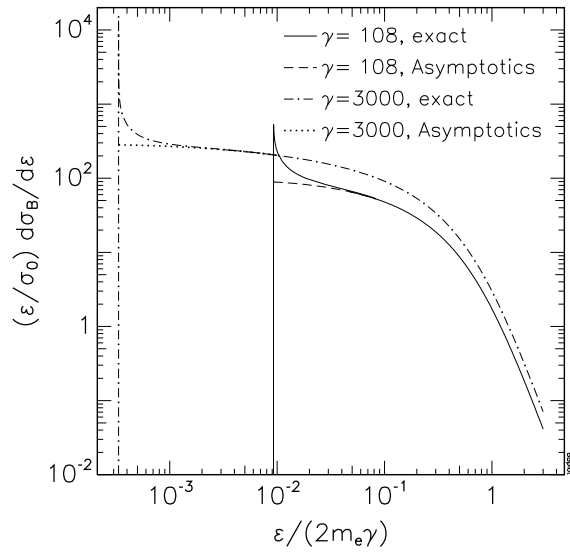


FIG. 5. The spectrum of the para-Ps as function of the scaled Ps energy $\varepsilon/(2m_e\gamma)$.